Structural and magnetic phase transitions of Fe on stepped Cu(111)

J. Shen, M. Klaua, P. Ohresser, H. Jenniches, J. Barthel, Ch. V. Mohan, and J. Kirschner
Max-Planck-Institut für Mikrostrukturphysik, Weinberg 2, 06120 Halle, Germany
(Received 19 May 1997)

The magnetism and its correlation with morphology and structure of ultrathin Fe/Cu(111) films have been studied. At room temperature, the films grow in a quasi-one-dimensional form (stripes) in the submonolayer range. Between 1.4 and 1.8 ML the stripes percolate and become two-dimensional films. The remanent magnetization of the percolated films was observed to be significantly more stable with respect to time than that of the stripes. At low thickness (<2.3 ML) the films adopt the fcc structure from the substrate and later transform to bcc(110) structure with Kurdjumov-Sachs orientation. Experimental evidence suggests that the fcc films have a low-spin ferromagnetic or ferrimagnetic phase, and a perpendicular easy magnetization axis. The magnetization switches to an in-plane high-spin phase after the fcc to bcc structural transformation has been accomplished. [S0163-1829(97)02541-1]

I. INTRODUCTION

The step decoration effect of Fe growth on Cu(111) has been noticed for some years since the first scanning tunneling microscopy (STM) study on this system.[1] Recently this effect has been used by the authors to produce one-dimensional (1D) Fe stripes on a stepped Cu(111) substrate.[2] It has been found that in the submonolayer regime the deposited Fe atoms form parallel stripes along the step edges. The magnetism of the stripes has a superparamagnetic nature which is distinguished from that of a two-dimensional (2D) ferromagnetic film mainly by its time-dependent remanent magnetization. Further increase in the thickness leads to an increase of the width of the stripes and finally results in the two-dimensional percolation of the films. This system has provided an opportunity to study the transition from 1D to 2D magnetism.

In addition the Fe/Cu(111) films have fcc structure in the low thickness limit,[3,4] which otherwise does not exist below 1100 K in bulk. The magnetism of fcc γ-iron appears to be very interesting. Theoretical calculations have shown that fcc γ-iron may be nonmagnetic, antiferromagnetic, low-spin, or high-spin ferromagnetic depending on the lattice parameters.[5] Though experimental evidence from the bulk indicates that fcc γ-Fe has a antiferromagnetic ground state,[6] the ultrathin films of γ-Fe on Cu(100) were observed to have a high-spin ferromagnetic phase at low thickness (<5 ML).[7] This high-spin ferromagnetic (FM) phase has been associated with the tetragonal distortion of the Fe fcc structure leading to an enlarged atomic volume.[8] To find out whether the high-spin FM phase is a general feature of 2D γ-Fe (ultrathin films), it is important to study the magnetic properties of γ-Fe on a copper substrate with another orientation, such as the (111) plane.

In contrast to the Fe/Cu(100) system, the structure and the magnetism of the Fe/Cu(111) system has been much less understood due to the very limited amount of work. So far it has been reported that at room temperature Fe grows pseudomorphically up to 4 or 5 monolayers,[4] and then transforms to the bcc structure with (110) orientation.[4,9–13] STM has shown that the growth of Fe on Cu(111) is in a three-dimensional manner at room temperature.[1,14] Magnetic measurements from a copper capped Fe/Cu(111) film suggested that the Fe has a surprisingly small magnetic moment ($\sim 0.6\mu$B).[11] The easy magnetization direction, however, appeared to depend strongly on the growth temperature.[11] An electron-capture spectroscopy study has reported the existence of long-ranged ferromagnetic order in a 4-ML film and short-ranged ferromagnetic order in one- or two-monolayer films.[15]

The aim of this work is to systematically study the structural and magnetic properties of the Fe/Cu(111) films with emphasis on the correlation between the structure and their magnetism. *In situ* STM, low-energy electron diffraction (LEED) with intensity vs energy function (I/V LEED) and magneto-optical Kerr effect (MOKE) have been used to study the thickness dependence of the morphology, atomic structure, and magnetism, respectively. The main results are summarized as follows.

(1) In the submonolayer range the Fe films have a quasi-1D form which is characterized by parallel aligned stripes. The remanent magnetization of the stripes was observed to be time dependent.

(2) Between 1.4 and 1.8 ML the Fe stripes percolate to form 2D films. The magnetization relaxation time of the 2D films is significantly longer than that of the 1D films.

(3) We proved the occurrence of the fcc to bcc transition. The critical thickness is between 2.3 and 2.7 ML, which is somewhat lower than the previously reported 4 or 5 ML.[4]

(4) The easy magnetization axis switches from perpendicular to in-plane between 2.3 and 3.0 ML, in coincidence with the fcc to bcc structural transition.

(5) In the fcc to bcc transformation regime, the magnetization of the Fe films sharply increases. The magnetization of the transformed bcc Fe films is about four to five times larger than the extrapolated value from the low thickness fcc Fe films.

The paper is organized as follows. We describe the experimental details in Sec. II. Sections III and IV present the structural and the magnetic results, respectively. The correlation between the observed structural and magnetic proper-

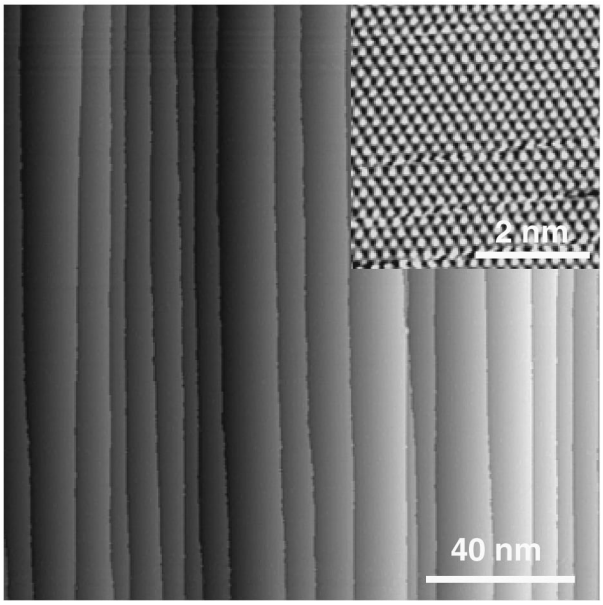

FIG. 1. STM topography image of a well-prepared Cu(111) vicinal surface. The atomic steps are parallel and oriented along ⟨011⟩ direction. The inset is an atomically resolved image ($I_t = 0.25$ nA, $V_{\text{bias}} = 10$ mV) recorded from a terrace showing the sixfold symmetry of the Cu(111) surface.

ties is discussed in Sec. V. The final conclusion will be drawn in Sec. VI.

II. EXPERIMENTAL DETAILS

The experiments were performed in a multichamber system including an MBE preparation chamber, an STM chamber, an analysis chamber equipped with facilities for Auger electron spectroscopy (AES), LEED and thin-film growth, and a MOKE chamber. The base pressure of the individual chambers is better than 5×10^{-11} mbar. The AES system has a cylindrical mirror analyzer (CMA) allowing the detecting limit to about 0.1 at. % for most of the elements. A fully automatic video-LEED system[16] has been used for recording LEED images as well as for measuring I/V LEED curves. In the present work the sample was prepared in the analysis chamber. The LEED and the AES measurements were taken immediately after film deposition. Then the sample was transferred to the MOKE chamber for magnetic measurements. STM images were recorded at room temperature after the MOKE study.

The copper substrate has a miscut of 1.2° with respect to the (111) orientation. The surface steps are aligned along one ⟨011⟩ direction with a (001) microfacet. The average terrace width is about 10 nm. Prior to film preparation the copper substrate was cleaned by Ar^+ sputtering and annealing cycles to 700 K. The crystallographic quality and the cleanliness of the substrate were monitored by LEED and AES, respectively. Both sharp LEED p(1×1) spots and the contamination-free Auger spectrum indicated the high quality of the substrate. The surface morphology of the substrate has also been examined by STM. As shown in Fig. 1, the surface consists of ⟨011⟩ oriented steps with an average terrace width of about 10 nm. The inset shows a magnified image with atomic resolution taken from a terrace region. The well-ordered atoms reflect the sixfold symmetry of the substrate surface, proving that the substrate surface is virtually defect free in the terraces.

The Fe films were prepared in the analysis chamber from an iron wire (5N in purity) heated by e-beam bombardment. At a typical Fe evaporation rate of 0.2 ML/min the pressure increased from 5×10^{-11} mbar to 1×10^{-10} mbar. To suppress interdiffusion, the copper substrate was kept at 0 °C during deposition.[17] Afterwards the sample was further cooled down to 170 K in order to avoid a temperature rise above 0 °C during transferring from the analysis chamber to the MOKE chamber.

In the MOKE chamber, the sample was placed on a manipulator with a function of three-axis movement as well as azimuthal rotation. The sample can be cooled down to 40 K and heated up to 600 K. In the present work most of the measurements were carried out in the sample temperature range between 90 and 270 K. Since the magnetization of nearly all the films persists above 270 K at which the interdiffusion starts to proceed, no attempts have been made to measure the Curie temperature in the present study. The polar and in-plane Kerr measurements are easily achieved by rotating the manipulator to allow the sample surface to be perpendicular or parallel to the external field. The maximum field is about 0.8 T, which appears to be large enough to saturate the films with thickness below 5 ML along the hard-axis direction.

III. MORPHOLOGY AND STRUCTURE

Figure 2 shows a series of STM topography images of Fe/Cu(111) films of different thickness. It is immediately visible that in the submonolayer regime (0.3 ML, 0.8 ML) the films have a quasi-1D form. The stripes are aligned parallel to one another on the upper edges of the steps. Most of the regions of the stripes have a monolayer height at 0.3 ML and increase to a double-layer height at 0.8 ML. At 0.3 ML the amount of Fe atoms is so small that the stripes are virtually formed by segments which are only weakly linked. At 0.8 ML, most of the segments have coalesced and the stripes become much more continuous. The edges of the stripes are rather rough. This is because the Fe atoms have a tendency towards growth along all three ⟨011⟩ directions even though they have a preferential alignment along the direction of the step edges. In other words, the Fe stripes are virtually formed by triangular-shaped islands which are linearly arrayed and connected. Such kind of construction of the stripes appears to have some strong influence on their magnetic properties, in particular the magnetization relaxation process which will be discussed in Sec. V.

With increasing thickness the stripes become wider and finally percolate between 1.4 and 1.8 ML, as seen in Figs. 2(c) and 2(d). This percolation leads to a direct connection between most of the stripes (>90%). In the present work we refer such a percolation as a 2D percolation while the connection between the segments within each stripe, i.e., between 0.3 and 0.8 ML, will be named 1D coalescence. Here the 2D percolation, in reality, leads to a 1D to 2D morphological transition of the films. The effect of this transition on the magnetism will also be discussed in Sec. V.

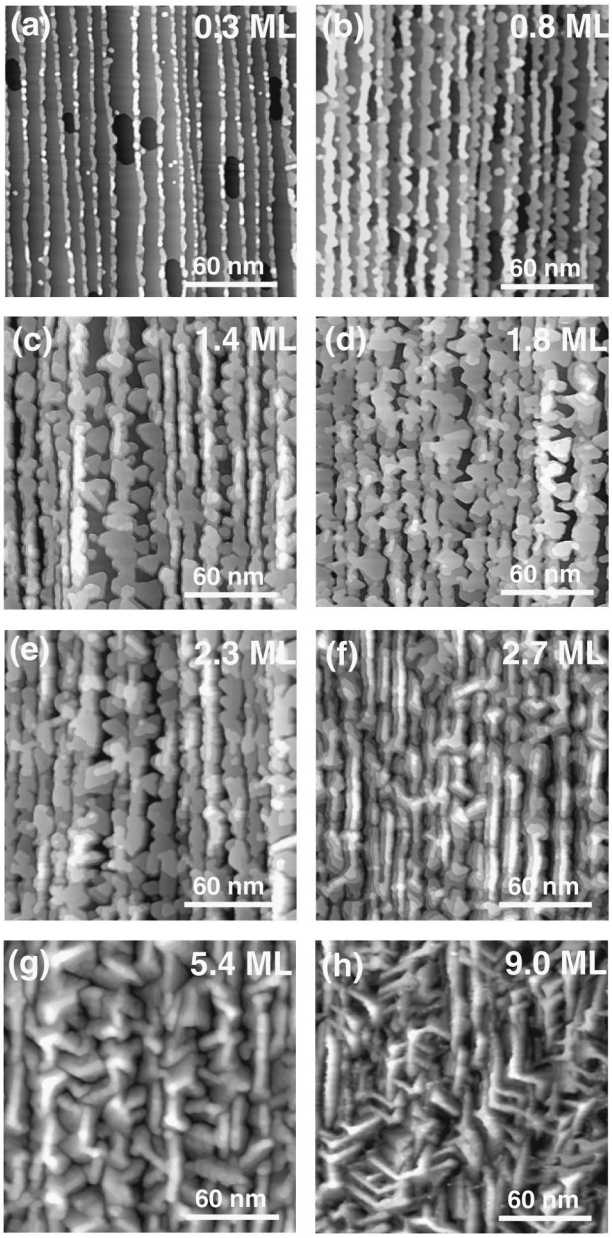

FIG. 2. Series of STM images showing the morphological evolution of the Fe/Cu(111) films with increasing thickness. In the submonolayer regime [(a) and (b)] the films have quasi-1D form. The 2D percolation occurs between 1.4 ML (c) and 1.8 ML (d). The morphology changes greatly between 2.3 ML (e) and 2.7 ML (f), as characterized by the formation of elongated domains aligning along the ⟨011⟩ directions.

Up to 2.3 ML the film morphology is characterized by triangular-shaped islands reflecting the threefold symmetry of the fcc (111) structure. As the islands are mostly bilayer or trilayer in height, the growth of the Fe/Cu(111) can be generally referred to as multilayer growth. Above 2.3 ML, the morphology of the films, however, changes significantly. The number of the exposed layers increases. It is 2 to 3 at 2.3 ML, 5 to 6 at 2.7 ML, and 7 to 8 at 9 ML. Moreover, the triangular-shaped islands are no longer visible in the images of the films with higher thickness [Figs. 2(e)–2(h)]. Instead some elongated domains appear which are aligned along the ⟨011⟩ directions. At 2.7 ML these domains are mainly oriented along the step direction. But those along the other two ⟨011⟩ directions gradually develop to become almost equally important (see the 9.0 ML image in Fig. 2).

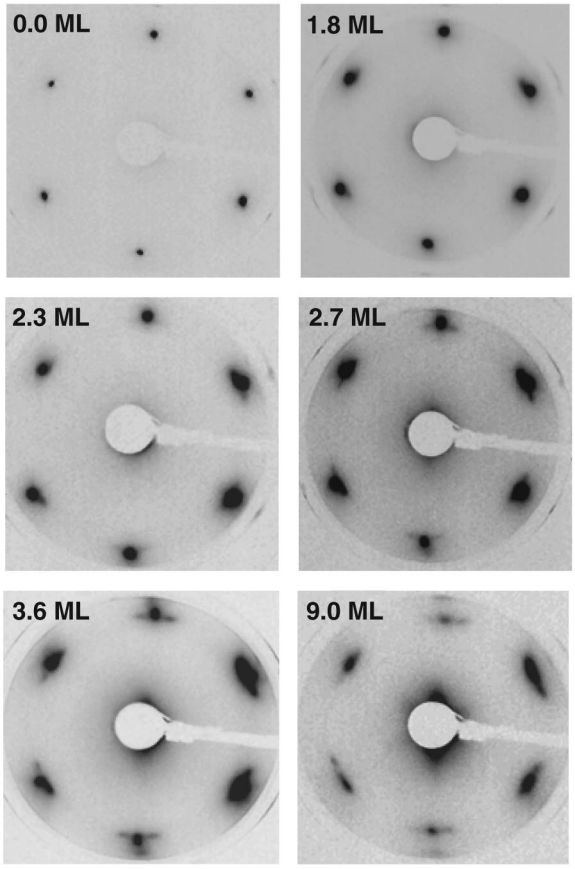

FIG. 3. LEED pattern of the Fe/Cu(111) films with different thickness. Below 2.3 ML the films have a p(1×1) pattern inherited from the substrate. From 2.3 ML on, satellite spots start to appear around the substrate spots. These satellite spots are caused by the bcc(110) domains with Kurdjumov-Sachs orientation.

The question immediately arises: what causes the changes of the film morphology in the thickness regime between 2.3 and 2.7 ML? Since the triangular shape of the islands is a reflection of the fcc(111) symmetry, losing this feature might imply losing the fcc(111) structure. Indeed, our LEED studies have proven that the films undergo a fcc to bcc structural transition between 2.3 and 2.7 ML. Figure 3 shows the LEED patterns taken from different films at about 65 eV. The 1.4-ML and the 1.8-ML films have p(1×1) patterns with respect to the clean copper substrate, indicating the pseudomorphic growth of the Fe films. Because of the increased roughness owing to the multilayer growth, the films show more diffuse LEED spots than the copper substrate. With increasing thickness some additional spots start to appear around the substrate spots. At 2.3 ML these spots are already visible though their intensity is very weak. At 2.7 ML or even higher thickness the LEED patterns are already featured by these additional spots. In fact, these satellite spots are better seen at the beam energy of about 90 eV, as shown in the upper-left picture of Fig. 4 for the 2.7-ML film. There appear to be five satellite spots around each substrate spot, with three in the inner circle and two in the outer circle. It

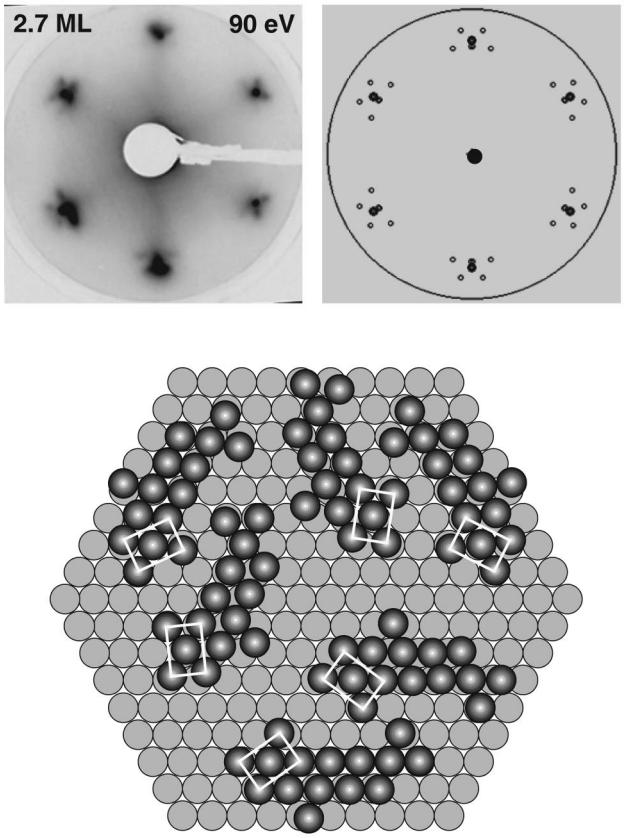

FIG. 4. Demonstration of the Kurdjumov-Sachs superstructure. Upper left: LEED pattern of the 2.7-ML film at the beam energy of 90 eV. Upper right: Simulated LEED pattern of Fe bcc(110) on Cu(111) with Kurdjumov-Sachs orientation. Note the consistency between the experimental and the simulated LEED patterns. Bottom: real-space schematic view of the six KS domains on the Cu(111) substrate.

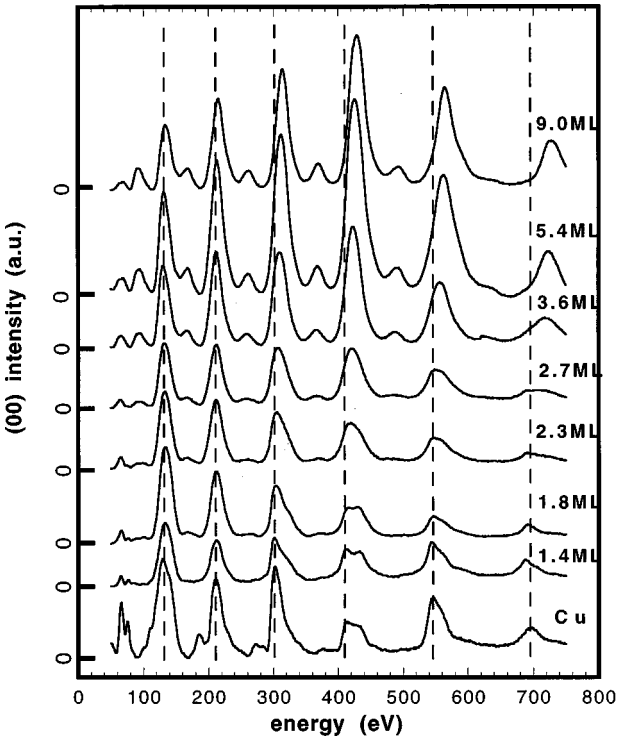

FIG. 5. IV-LEED spectrum of the (00) beam for the Fe/Cu(111) films. The 0's on the y axis indicate the zero level of the intensity of the corresponding curves after background subtraction. Below 2.3 ML there is no distinct peak shift. At higher thickness the peaks shift towards higher energies. The dashed lines indicate the peak position of the substrate.

has already been discussed in previous work that these spots result from the bcc(110) domains in Kurdjumov-Sachs (KS) orientation.[4] The KS orientation is a special case of the one-dimensional matching between bcc (110) and fcc(111) (bcc [111] is parallel to fcc [101]) with sides of the rhombic unit meshes of the film and the substrate to be parallel. Using the bulk parameters of Fe and Cu, we have simulated the LEED pattern of the KS orientation which is shown in the upper-right of Fig. 4. Except the middle two spots in the inner circle of the simulated pattern which are too close to be resolved experimentally, the experimental and the simulated LEED patterns agree well with each other. The six satellite spots reflect the six kinds of atomic relationship between the bcc(110) and fcc(111) structure as shown in the bottom picture of Fig. 4. Since these KS domains have only a one-dimensional matching with the substrate, each domain tends to have a narrow width in order to reduce the stress. In principle these six domains should have no preference on a flat surface due to the sixfold symmetry of the surface. Owing to the mirror symmetry, there are two kinds of domains along each ⟨011⟩ direction. As a result, the morphology of the films could be viewed as ridgelike structures oriented along the three ⟨011⟩ directions on a similar number. However, the STM images have shown that there are more domains elongated along the step direction than the other two ⟨011⟩ directions [see the 2.7-ML image in Fig. 2(f)]. This can be explained by the fact that the substrate steps are oriented only in one of the ⟨011⟩ directions and therefore have introduced a twofold symmetry in addition to the sixfold symmetry of the fcc(111) surface. The two domain configurations which are parallel to the steps should be more favored as compared to the other four domains. The dominance of the two particular KS domains should, in principle, make the corresponding satellite spots have different intensity as compared to the rest satellite spots. However, as a result of the limited resolution and the rather rough surface, it is difficult to conclude this from our LEED data.

The structural transition from fcc to bcc is further analyzed by an IV-LEED study of the system. Figure 5 shows the (00) beam intensity vs energy curves for films with different thickness. These curves were obtained with the incident angle of the primary beam to be about 6° off the surface normal. In this case the step direction of the substrate is perpendicular to the plane of incidence. The dashed lines in Fig. 5 mark the peak position of the copper substrate. It is evident that with increasing thickness up to 2.3 ML there is no major shift of the peak position. There seems to be only one family of peaks inherited from the substrate (fcc), which is in stark contrast to the Fe/Cu(100) system where two families of peaks have been observed corresponding to fcc and fct, respectively.[8] Above 2.7 ML, the peaks have clearly shifted towards higher energies. Such a shift, within the kinematic approximation, indicates that the average interlayer distance of the films becomes smaller than that of the substrate. Using the kinematical model, we have calculated the

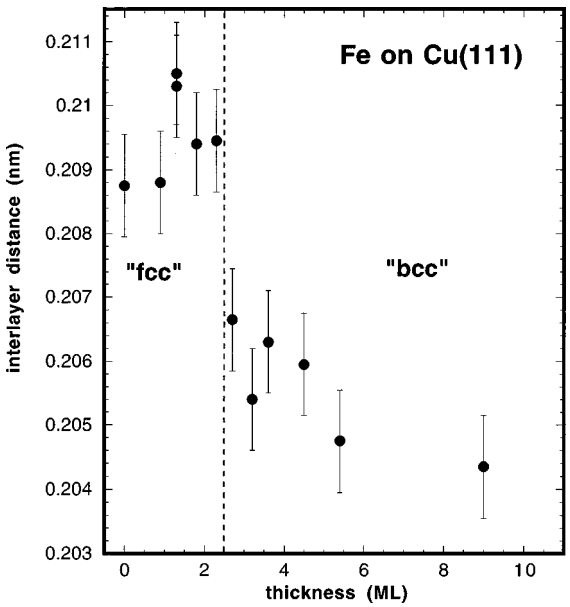

FIG. 6. The calculated interlayer distance from Fig. 5 using the kinematic approximation. It is evident that the interlayer distance decreases above 2.3 ML. The vertical dashed line separates films with different LEED structure. The films have a fcc-like structure below 2.5 ML, and a bcc structure above.

interlayer distance as a function of the film thickness. The results are shown in Fig. 6. Two regions can be clearly distinguished as indicated by the dashed line: in the low thickness region where the films show a p(1×1) pattern the interlayer distance of the films is close to that of the copper substrate, while in the high thickness region the interlayer distance of the films becomes apparently smaller. However, it has to be noted that the accuracy of the absolute value by our determination is influenced by the simple kinematic model, as the deviation of the calculated interlayer distance from the corresponding bulk value is about 0.001 and 0.003 nm for the fcc(111) and bcc(110), respectively. Nevertheless, the fact that the interlayer distance of the films drops down between 2.3 and 2.7 ML by more than 0.002 nm is quite unambiguous. This decrease of the interlayer distance is consistent with the LEED patterns which indicate the fcc to bcc structural transition between 2.3 and 2.7 ML.

The observed critical thickness of the fcc→bcc transformation is smaller than the previously reported value[4] of about 4 or 5 ML. This might be due to the fact that a vicinal copper substrate is used in the present work. Compared to the growth of Fe on a flat substrate, at the same nominal thickness the step decoration effect of the Fe growth on the vicinal substrate could make the films be locally thicker along the step edges. The fcc→bcc transformation could proceed first in these locally thicker regions. In addition, on the vicinal surface the islands have an elongated shape along one of the ⟨011⟩ directions (the step direction) even before the structural phase transformation. These elongated islands may have an easier path to convert into bcc KS domains as compared to the normal triangular-shaped islands on a flat Cu(111) surface. This is in fact backed by our STM observations that the bcc domains along the step direction appears earlier than those along the other two ⟨011⟩ directions. In Fig. 2 we have shown that at the beginning of the transformation (about 2.7 ML) most of the bcc domains are oriented along the step direction. The number of the bcc domains oriented along the other two ⟨011⟩ directions only become significant at higher thickness (e.g., see the 5.7-ML image in Fig. 2). Therefore, it is not surprising that the Fe films on the vicinal Cu(111) substrate transform into bcc structure at lower thickness than the films on a flat Cu(111) substrate.[18]

IV. MAGNETIC PROPERTIES

As shown in Fig. 2, in the submonolayer regime the Fe/Cu(111) films have a quasi-1D form. In our previous polar MOKE measurements we have shown that these Fe stripes exhibit hysteresis with a coercivity depending strongly on the temperature.[2] The easy magnetization axis of the stripes is determined to be perpendicular to the surface, because no magnetic signal was detected in the longitudinal geometry, irrespective of the external field being parallel or perpendicular to the stripes. In the same work we have also performed time-dependent magnetization measurements by MOKE. The results obtained from the stripes, which has a submonolayer nominal coverage (~0.8 ML), showed that at zero field the magnetization decays at a speed strongly depending on the temperature. For example, while the magnetization of the 0.8-ML stripes decays very slowly at about 100 K, it decays rapidly to zero (within 20 sec) at 160 K. We associated the decay of the magnetization with the superparamagnetic nature of the 1D stripes. The fact that the superparamagnetic stripes exhibit hysteresis is simply because the measuring time of the magnetization curves is considerably shorter than the magnetization relaxation time of the stripes.

Here we extend the previous work by demonstrating the coverage-dependent magnetization relaxation process of the Fe/Cu(111) films. Figure 7 shows the magnetization relaxation curves of films with different thickness ranging from that of the 1D stripes to the 2D percolated film. All the curves were measured in the polar geometry. The 0 level of each curve indicates the signal of a demagnetized state of the films. An external field of about 0.6 T was applied at the time point which is marked as ''field on.'' For all the films the magnetization quickly reaches saturation. The external field was removed at the time point marked as ''field off.'' In all three cases the magnetization falls down, but with distinctly different speed. At 160 K, the magnetization of the 0.8-ML film decays down to zero within 20 sec. In contrast, at the same temperature after an initial quick decay the residual magnetization of the 2-ML film is much more stable. The quickest decay of the magnetization is observed, however, for the 0.3-ML film. Its magnetization decays rapidly to zero in a few seconds even at much lower temperature of 50 K. The different behavior of the magnetization relaxation process of these films appears to be closely correlated with their morphology, which will be discussed in the next section.

We now turn to consider the magnetic anisotropy of the Fe/Cu(111) films. As mentioned above, the easy magnetization axis of the submonolayer films (the stripes) is perpendicular to the film surface. This in fact has been found to be the case for all the films below 2.3 ML of thickness. Figure 8 shows the magnetization curves of films measured in both polar (a) and longitudinal (b) geometry. It is evident that

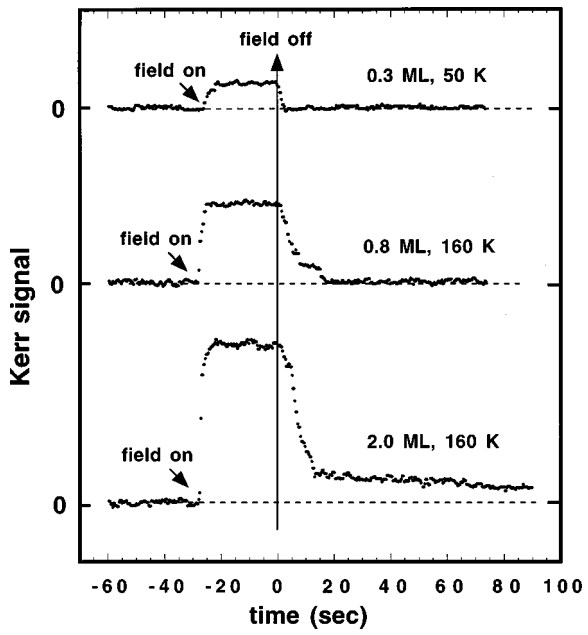

FIG. 7. Time dependence of the magnetization of the Fe/Cu(111) films at different thickness. At the same temperature of 160 K, after removal of the field the decay of the magnetization of the 2-ML film is significantly slower than that of the 0.8-ML film. The magnization of the 0.3-ML film decays rapidly to zero at an even lower temperature of 50 K.

below 2.3 ML the films exhibit magnetic signals only in the polar geometry, indicating that the easy magnetization direction is perpendicular to the surface. At 160 K, the polar hysteresis loops of the films ($<$2.3 ML) are usually characterized by small remanence and coercivity. On the scale of the lower panel of Fig. 8(a), the hysteresis of the loops is virtually invisible. The loop of the 2.0-ML film has been magnified in the upper panel of Fig. 8(a), where a clear hysteresis can be seen. With increasing thickness, the saturation field increases from 400 Oe for the 2.0-ML film to 850 Oe for the 2.5-ML film. The 2.3- and 2.5-ML films, as shown in Fig. 8(b), start to exhibit weak magnetic signals in the in-plane geometry. Further increasing thickness up to 3.0 ML, the in-plane magnetization curves become much more pronounced with a near rectangular shape. The perpendicular magnetization, on the other hand, becomes much harder to saturate. The saturation field for the 3.0-ML film is about 4500 Oe, a value which is almost five times larger than that of the 2.5-ML film. This indicates that at a thickness of 3.0 ML or higher the easy magnetization axis lies parallel to the surface. We therefore conclude that the easy magnetization direction switches from perpendicular to in plane in the thickness range between 2.3 and 3.0 ML.

The films with in-plane easy magnetization axis ($>$3.0 ML) have the bcc structure with KS orientation. Without the step-induced twofold symmetry, the magnetization curves should be identical if measured along the three $\langle 011 \rangle$ directions. Due to the existence of the well-aligned steps, the step direction is no longer equivalent to the other two $\langle 011 \rangle$ directions. We have observed (not shown here) that it requires a larger field to saturate the films along the step direction than along the other two $\langle 011 \rangle$ directions. At this stage it is not possible for us to determine the anisotropy direction in

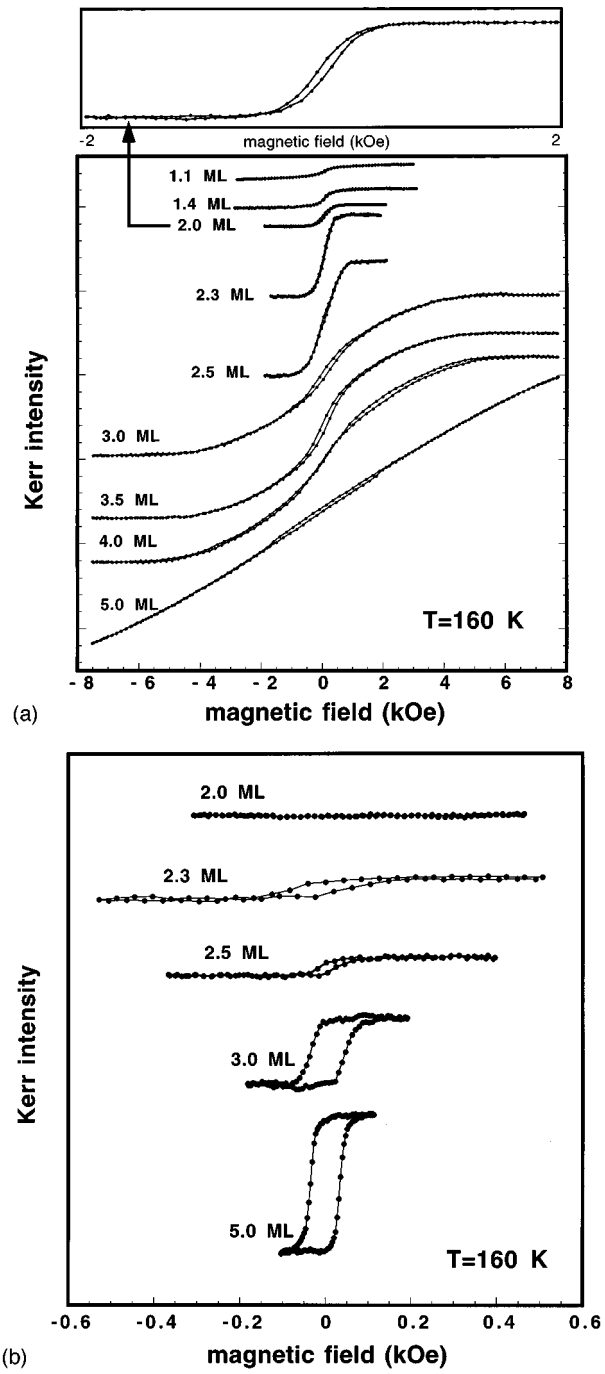

FIG. 8. The magnetization curves of films with increasing thickness. (a) Polar curves. (b) In-plane curves. Below 2.3 ML, the magnetic signal can only be detected in the polar geometry. The upper panel in (a) shows a magnified loop of the 2-ML film. When increasing thickness from 2.5 ML to 3.0 ML, the saturation field in the perpendicular direction greatly increases by a factor of 5. The in-plane signal starts to appear at 2.3 ML, and at 3.0 ML already develops to a well-defined rectangular loop.

the plane because of the limited azimuthal angles we were able to cover presently. Instead, we can conclude that the easy magnetization axis is at least not along the step direction.

We also want to point out a remarkable change of the magnetism in the thickness range from 2.3 to 3.0 ML, that is the rapid increase of the saturation Kerr signal. Figure 9

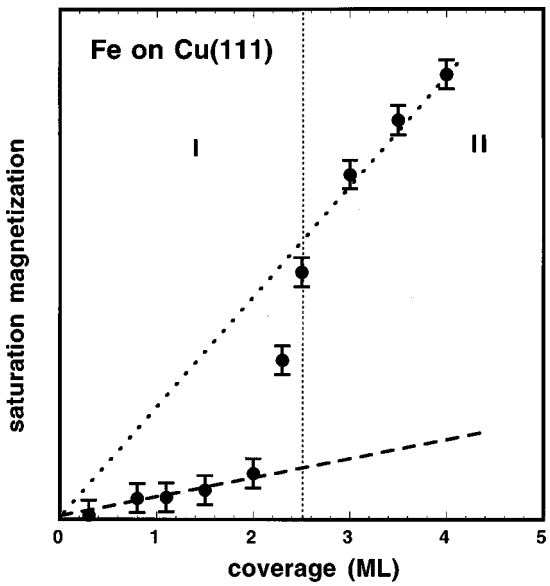

FIG. 9. The saturation magnetization as a function of film thickness. The measuring temperature is about 160 K. The magnetization abruptly increases about four to five times at the crossover from region I to II which is indicated by the vertical line. The vertical line marks the thickness at which the LEED pattern changes from fcc to bcc structure. The magnetization of both the fcc Fe films and the bcc Fe films increases linearly with thickness. Note the slope of the bcc films' magnetization (dotted line) to be about five times larger than that of the fcc films (dashed line).

shows the saturation Kerr signal as a function of the film thickness. Note all the films were saturated along the surface normal no matter whether their easy magnetization axis is perpendicular or parallel to the surface. Below 2.3 ML, the Kerr signals of the films have small values whose linear extrapolation (dashed line) extends approximately through zero. With increasing thickness the Kerr signals of the films, in principle, should lie on the dashed line if the magnetic moment of the films keeps constant. However, Fig. 9 clearly indicates that between 2.3 and 3.0 ML the measured Kerr signals increase much quicker than just linearly. Structurally this thickness range is exactly that of the fcc to bcc transformation. After the completion of the structural transformation ($>$3.0 ML), the Kerr signals of the bcc films increases again more or less linearly as indicated by the dotted line. The slope of the dotted line, however, is about five times larger than that of the dashed line. This means that the Kerr signals of the bcc films are about five times larger than expected from the linear extrapolation of the dashed line. The origin of this unusual increase of the Kerr signal as well as the spin reorientation will be discussed in the following section.

V. CORRELATION BETWEEN MORPHOLOGY, STRUCTURE, AND MAGNETISM

In this section we discuss the magnetic properties of the Fe/Cu(111) films at the morphological and the structural level. The first thing to note is that the magnetization relaxation time of the 0.3-, 0.8-, and 2-ML films increases significantly with increasing thickness (Fig. 7). Meanwhile, these films are distinctly different in terms of the morphological percolation status. The 0.3-ML film is below 1D coalescence. Its stripes are formed by short segments which are weakly linked or even disconnected. The 0.8-ML film, however, has a thickness above 1D coalescence, and the stripes are much more continuous. In the previous work we have already discussed the superparamagnetic nature of these quasi-one-dimensional stripes.[2] Each stripe is divided into some superparamagnetic spin blocks. Although inside each block the spins are ferromagnetically coupled, the spin blocks are more or less independent from each other with only weak coupling between them. The volume of the spin blocks (V_b) can be obtained by fitting the measured hysteresis curves. The fitted V_b of the 0.3-ML film was found to be close to the volume of the segments. This is not surprising since the links between the segments are weak. The somewhat surprising result is that the fitted V_b of the 0.8-ML film was found only about four times larger than that of the 0.3-ML film, though the stripes of the 0.8-ML film are rather continuous. We believe this is mainly due to the rough edge of the stripes, which results in some weak connections along the stripes. According to the Néel model,[19] the superparamagnetic relaxation time exponentially increases with the increase of the volume of the block unit. This explains why the relaxation time of the 0.8-ML film is longer than that of the 0.3-ML film, even though the later was measured at a much lower temperature of 50 K. The 2-ML film, on the other hand, is already a percolated 2D film, since the two-dimensional percolation occurs between 1.4 and 1.8 ML. The 2D percolation of the films may lead to a significantly more stable remanent magnetization by two possible mechanisms: (1) the films are still superparamagnetic but with a much longer relaxation time; (2) a true long-range order has already been built up in the films. It is not clear which mechanism holds in this particular case, though the fact that the remanence of the 2-ML film slowly decays may imply a superparamagnetic nature of the film. Nevertheless, the island size of the 2-ML film should be much larger than that of the other two films because of the 2D percolation. Therefore the 2-ML film has the longest relaxation time among the films shown in Fig. 7.

Despite of their superparamagnetic nature, all the films below 2.3 ML have an easy magnetization axis perpendicular to the surface. At the low thickness limit the sign of the effective anisotropy constant is usually governed by the surface anisotropy constant (K_s). This implies that the surface anisotropy of the Fe/Cu(111) system favors perpendicular magnetization. With increasing thickness above 2.3 ML the spin reorientation starts to take place. The origin of this spin reorientation may come from two factors. The first one is the interplay between the positive surface anisotropy and the negative shape anisotropy. Since the surface anisotropy remains constant with increasing thickness while the shape anisotropy increases, it is expected that above a certain critical thickness the easy magnetization axis will switch from perpendicular to in plane. The second one is the structural transformation from fcc(111) to bcc(110), which occurs in almost the same thickness regime as the spin reorientation. The twofold in-plane symmetry of the bcc(110) plane provides an in-plane anisotropy in addition to the usual perpendicular anisotropy. The film thus may have a in-plane easy magnetization axis once the bcc(110) structure is attained. Such fcc to bcc structural transformation-induced spin reorientation

has also been observed in the Fe/Cu(100) system.[20] There has been no direct proof which of the above two factors is playing the dominant role, but the critical thickness of the fcc→bcc structural transformation and the spin reorientation agrees so well that it is unlikely to be only an accidental matching.

There has also been a report on the temperature-dependent spin reorientation in the Fe/Cu(100) system,[21] where the magnetization reversibly switches from perpendicular (low temperature) to in plane (high temperature). A similar study has not been thoroughly carried out in the present Fe/Cu(111) system, because the LN_2 cooling in the MOKE is limited to about 150 K. Above this temperature no temperature-dependent spin reorientation has been observed in the critical thickness regime. It would be interesting to study whether such a phenomenon occurs at a lower temperature, which is important to understand the origin of the spin reorientation in this system.

The fcc to bcc structural transformation is accompanied not only by the spin reorientation, but also by the abrupt increase of the saturation Kerr signals of the films by four to five times (Fig. 9). Since the MOKE does not measure the magnetization directly, we have to first discuss whether the sudden increase of the measured Kerr signal is caused just by the different optical response of the fcc and the bcc films. For this we have measured the Kerr intensity of a high-spin 3.4-ML fcc Fe/Cu(100) film and a 3.5-ML bcc Fe/Cu(111) film. To compare the Kerr intensity contributed from an individual atom, one has to consider that the atomic density of the (111) face is about 15% higher than that of the (100) face. Thus we have scaled the measured Kerr intensity by the corresponding coverage and atomic density. The results are shown in Fig. 10. Apparently the results indicate that there is no major difference between the optical response of the fcc and the bcc Fe films. The scaled Kerr intensity of the fcc Fe/Cu(100) film seems to be slightly larger than that of the bcc Fe/Cu(111) film, which probably reflects the fact that the magnetic moment of the high-spin fcc Fe, i.e., between 2.4 and $2.7\mu B$,[22,23] is somewhat larger than that of the bcc Fe ($\sim 2.2\mu B$). Therefore the measured Kerr intensity from both fcc and bcc films, to first order, is proportional to the magnetization. Assuming the transformed bcc Fe films to be uniformly magnetized with the magnetic moment equal to that of the bulk, one has to assume that either the fcc Fe/Cu(111) films are nonuniformly magnetized with 70–80 % of the films to be nonferromagnetic, or the films are in a ferrimagnetic state, or these films are uniformly magnetized but have a low-spin FM phase whose moment is about four to five times smaller than that of the bcc Fe. The first assumption appears to be unlikely since the IV-LEED spectrum shows the films to have only one family of fcc peaks. This means that there is no distinct difference between the interlayer distance of different layers. Furthermore, Fig. 9 shows that the 1-ML film also has a low magnetization. Since the 1-ML film has only two layers in height distribution, to assume more than 70% of such a perpendicularly magnetized film is nonferromagnetic implies that one of its two layers is partly ferromagnetic and partly nonferromagnetic (the other layer is nonmagnetic). Such a magnetic configuration can only be possible if the film has different structure or composition within the same layer. However, both the STM and the LEED studies indicate that the films have uniform structure within one layer.

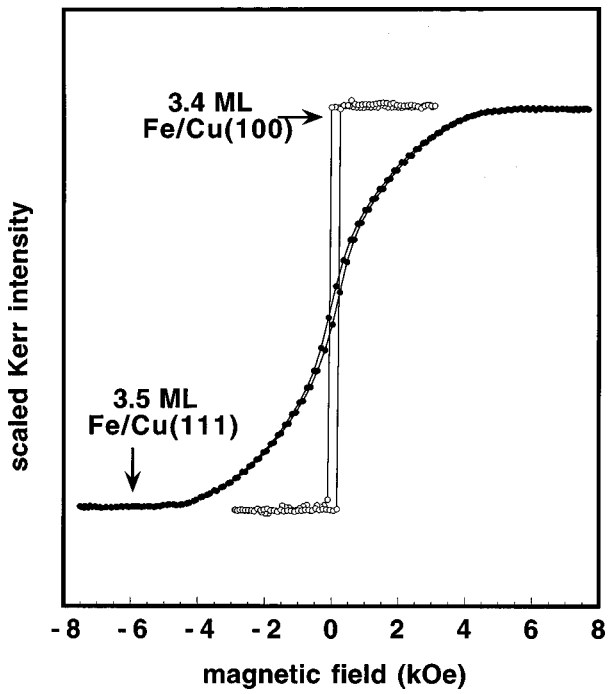

FIG. 10. Comparison of the polar Kerr hysteresis loops of a 3.4-ML fcc Fe/Cu(100) film and a 3.5-ML bcc Fe/Cu(111) film. Both loops were measured at 160 K. The Kerr intensity of the two films has been scaled by the corresponding coverage and atomic density. As the magnetic moment of the two films is close, it is clear that the optical response of the fcc and the bcc Fe films is virtually the same.

The possible existence of ferrimagnetism in fcc Fe has been predicted by Zhou *et al.* in a recent theoretical calculation.[24] The authors have pointed out that for lattice constants from 3.59 to 3.67 Å, fcc Fe could have a ferrimagnetic configuration with a net moment to be about 0.3 to $0.4\mu B$. If we assume the transformed bcc Fe films (>3.0 ML) to have the bulk moment of $2.2\mu B$, the fcc Fe/Cu(111) films should have a moment of about 0.4 to $0.5\mu B$, which is not far from the theoretical value. In this respect one may not rule out the possibility that the fcc Fe/Cu(111) films are in a ferrimagnetic state. However, we seem to have some experimental evidence suggesting that the ferrimagnetic alignment of the spins must be within each (111) plane rather than between the planes. This is because the 0.3-ML film (see Fig. 9), which is formed only by monolayer-high islands, is also in a low-moment magnetic state. A possible spin alignment within a particular fcc(111) layer would be the following: the two corner spins on the long diagonal axis of the rhombic unit cell are in the reverse direction (up) as compared to the two corner spins (down) on the short diagonal axis. This would lead the net magnetization to be 1/3 of the total magnetization with the assumption that each spin has the same absolute value of the moment. To our knowledge, there has been no theoretical work discussing such a spin alignment of the fcc Fe. Therefore this model is yet to be proven by theoretical calculations.

A more likely option is that the fcc Fe/Cu(111) films are in the low-spin (LS) ferromagnetic phase. Theoretical calcu-

lations indicate that there exist two LS phases, LS1 and LS2.[22–24] The magnetic moment is about 0.9–1.5μB for LS1, and no larger than 0.4μB for LS2. The estimated moment from our data is about 0.4 to 0.5μB, which is closer to the calculated value of the LS2 phase. In fact, in their early work Gradmann *et al.*[11] have reported a moment value of about 0.5–0.6μB from a copper capped Fe/Cu(111) film. The agreement seems to indicate that the copper capping does not affect the magnetic moment strongly. The low moment of the fcc Fe(111) films has its structural base, as evidenced from our experiments. As shown in Fig. 6, in the fcc thickness regime the interlayer distance of the Fe films is nearly the same as that of the copper substrate. Therefore, unlike the case of Fe/Cu(100), the Fe/Cu(111) films have no significant tetragonal distortion and thus no enlargement of the atomic volume. The relatively smaller atomic volume of the Fe/Cu(111) films, according to theory,[5] leads to a low-spin FM phase.

However, it is puzzling why the high-spin FM phase is only revealed in the Fe/Cu(100) system but not in the Fe/Cu(111) system. An equivalent question from the structural point of view is why the same lattice mismatch leads to a completely different tetragonal distortion in the two systems. A plausible explanation is that the driving force of the tetragonal distortion in these two systems is different. Since both of the systems transform to the bcc(110) phase at high thickness, it is possible that the Fe films, even in the fcc regime, tend to have an interlayer distance close to that of bcc(110). The interlayer distance of fcc Cu(100), fcc Cu(111), and bcc Fe(110) are 0.181, 0.208, 0.201 nm, respectively. If the above assumption is correct, the Fe/Cu(100) films should have an expanded interlayer distance while the Fe/Cu(111) films will have no tendency towards expansion. This appears to be consistent with the experimental observations of the two systems.

Another possible mechanism is that the strain in the two systems becomes different due to the morphology. The Fe/Cu(100) system has a much smoother surface as compared to that of the Fe/Cu(111). The significantly higher step density in the Fe/Cu(111) system may lead to a relaxation of the strain. In fact, such strain relaxation by the step edge atoms has already been observed in the Co/Cu(100) and Cu/Cu(100) system.[25] The different strain, however, could well lead to a different vertical expansion of the films. It would be interesting to find a way to prepare the Fe/Cu(111) films with smooth surface and compare their magnetization with the values in Fig. 9. The conventional way of annealing will cause a significant intermixing between Fe and Cu which can even ''kill'' the magnetism of the Fe films.[26] Recently Camarero *et al.*[27] have succeeded in using the surfactant Pb to improve the 2D growth of Co on Cu(111). This has given great hope of achieving smooth Fe/Cu(111) films with a similar method.

VI. CONCLUSIONS

In conclusion, we have studied the morphology, structure, and magnetism of Fe films on a stepped Cu(111) substrate. In the submonolayer regime the Fe films have a quasi-1D form characterized by stripes along the step edges. The stripes percolate between 1.4 and 1.8 ML, above which the films start to have a 2D form. The 2D percolation leads to a significantly more stable remanent magnetization. Between 2.3 and 2.7 ML the film undergoes a structural transition from fcc(111) to bcc(110) with Kurdjumov-Sachs superstructure. In the thickness region between 2.3 and 3.0 ML, the easy magnetization axis switches from perpendicular to in plane. This spinreorientation is probably associated with the structural phase transformation from fcc to bcc. Experimental evidence also strongly suggests that the Fe films have a low-spin FM phase in the fcc thickness regime, which is clearly distinguished from the high-spin FM phase in the bcc thickness regime.

ACKNOWLEDGMENTS

The authors are grateful to Dr. H. P. Oepen for valuable discussions. We would also like to thank F. Pabisch and G. Kroder for their technical support.

[1] A. Brodde and H. Neddermeyer, Ultramicroscopy **42-44**, 556 (1992); A. Brodde, K. Dreps, J. Binder, Ch. Lunau, and H. Neddermeyer, Phys. Rev. B **47**, 6609 (1993).
[2] J. Shen, R. Skomski, M. Klaua, H. Jenniches, S. Sundar Manoharan, and J. Kirschner, Phys. Rev. B **56**, 2340 (1997).
[3] U. Gradmann and P. Tillmann, Phys. Status Solidi A **44**, 539 (1977).
[4] D. Tian, F. Jona, and P. M. Marcus, Phys. Rev. B **45**, 11 216 (1992).
[5] V. L. Moruzzi, P. M. Markus, and J. Kubler, Phys. Rev. B **39**, 6957 (1989).
[6] S. C. Abrahams, L. Cuttman, and J. S. Kasper, Phys. Rev. **127**, 2052 (1962).
[7] R. D. Ellerbrock, A. Fuest, A. Schatz, W. Keune, and R. A. Brand, Phys. Rev. Lett. **74**, 3053 (1995).
[8] S. Müller, P. Bayer, C. Reischl, K. Heinz, B. Feldmann, H. Zillgen, and M. Wuttig, Phys. Rev. Lett. **74**, 765 (1995).
[9] U. Gradmann, W. Kümmerle, and P. Tillmanns, Thin Solid Films **34**, 249 (1976).
[10] W. Kümmerle and U. Gradmann, Solid State Commun. **24**, 33 (1977).
[11] W. Kümmerle and U. Gradmann, Phys. Status Solidi A **45**, 171 (1978).
[12] Y. Darici, J. Marcano, H. Min, and P. A. Montano, Surf. Sci. **195**, 566 (1988).
[13] M. T. Kief and W. F. Egelhoff, Jr., J. Vac. Sci. Technol. A **11**, 1661 (1993).
[14] H. Jenniches, M. Klaua, H. Höche, and J. Kirschner, Appl. Phys. Lett. **69**, 3339 (1996).
[15] C. Rau, C. Schneider, G. Xing, and K. Jamison, Phys. Rev. Lett. **57**, 3221 (1986).
[16] J. Giergiel, H. Hopster, J. M. Lawrence, J. C. Hemminger, and J. Kirschner, Rev. Sci. Instrum. **66**, 3474 (1995).
[17] M. Klaua, H. Höche, H. Jenniches, J. Barthel, and J. Kirschner, Surf. Sci. **381**, 106 (1997).
[18] Our recent LEED studies on Fe films grown on a flat Cu(111) crystal have proved that the films indeed transform to the bcc structure at higher thickness.

[19] L. Néel, Ann. Geophys. **5**, 99 (1949).
[20] J. Thomassen, F. May, B. Feldmann, M. Wuttig, and H. Ibach, Phys. Rev. Lett. **69**, 3831 (1992).
[21] D. P. Pappas, K.-P. Kämper, and H. Hopster, Phys. Rev. Lett. **64**, 3179 (1990).
[22] J. Kubler, Phys. Lett. **81A**, 81 (1981).
[23] C. S. Wang, B. M. Klein, and H. Krakauer, Phys. Rev. Lett. **54**, 1852 (1985).
[24] Yu-mei Zhou, Wen-qing Zhang, Lie-ping Zhong, and Ding-sheng Wang, J. Magn. Magn. Mater. **145**, L273 (1995).
[25] J. Fassbender, U. May, B. Schirmer, R. M. Jungblut, B. Hillebrands, and G. Güntherodt, Phys. Rev. Lett. **75**, 4476 (1995).
[26] J. Shen, M. Klaua, and J. Kirschner (unpublished).
[27] J. Camarero, T. Graf, J. J. de Miguel, R. Miranda, W. Kuch, M. Zharnikov, A. Dittschar, C. M. Schneider, and J. Kirschner, Phys. Rev. Lett. **76**, 4428 (1996).